Supplement of Earth Syst. Sci. Data, 18, 6171–6189, 2026
https://doi.org/10.5194/essd-18-6171-2026-supplement

Open Access Earth System Science Data

Supplement of

TCOM-CFC11 and TCOM-CFC12: a gap-free, observationally constrained global dataset of stratospheric CFC-11 and CFC-12 profiles (v2.0)

Sandip S. Dhomse and Martyn P. Chipperfield

Correspondence to: Sandip S. Dhomse (s.s.dhomse@leeds.ac.uk)

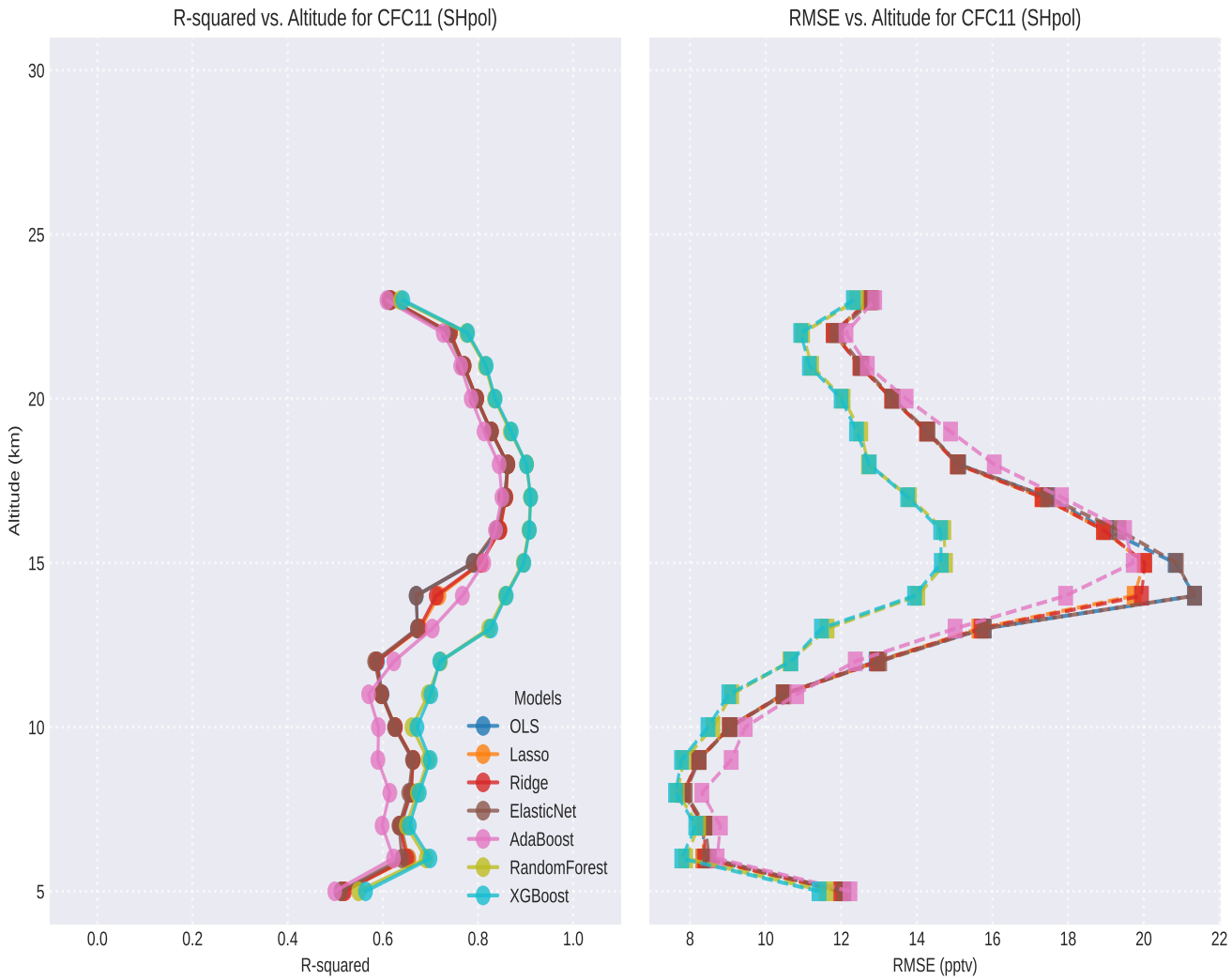

Figure S1. Vertical profiles of the goodness of fit (R^2) and Root Mean Squared Error (RMSE) for CFC-11 in the Southern Hemisphere Polar (SHpol, 90°S to 50°S) latitude bin. The metrics are derived from a comparative analysis of seven regression models: OLS, Lasso, Ridge, ElasticNet, AdaBoost, RandomForest, and XGBoost. Overall, the XGBoost model demonstrates superior predictive accuracy and robustness, particularly within the stratospheric levels.

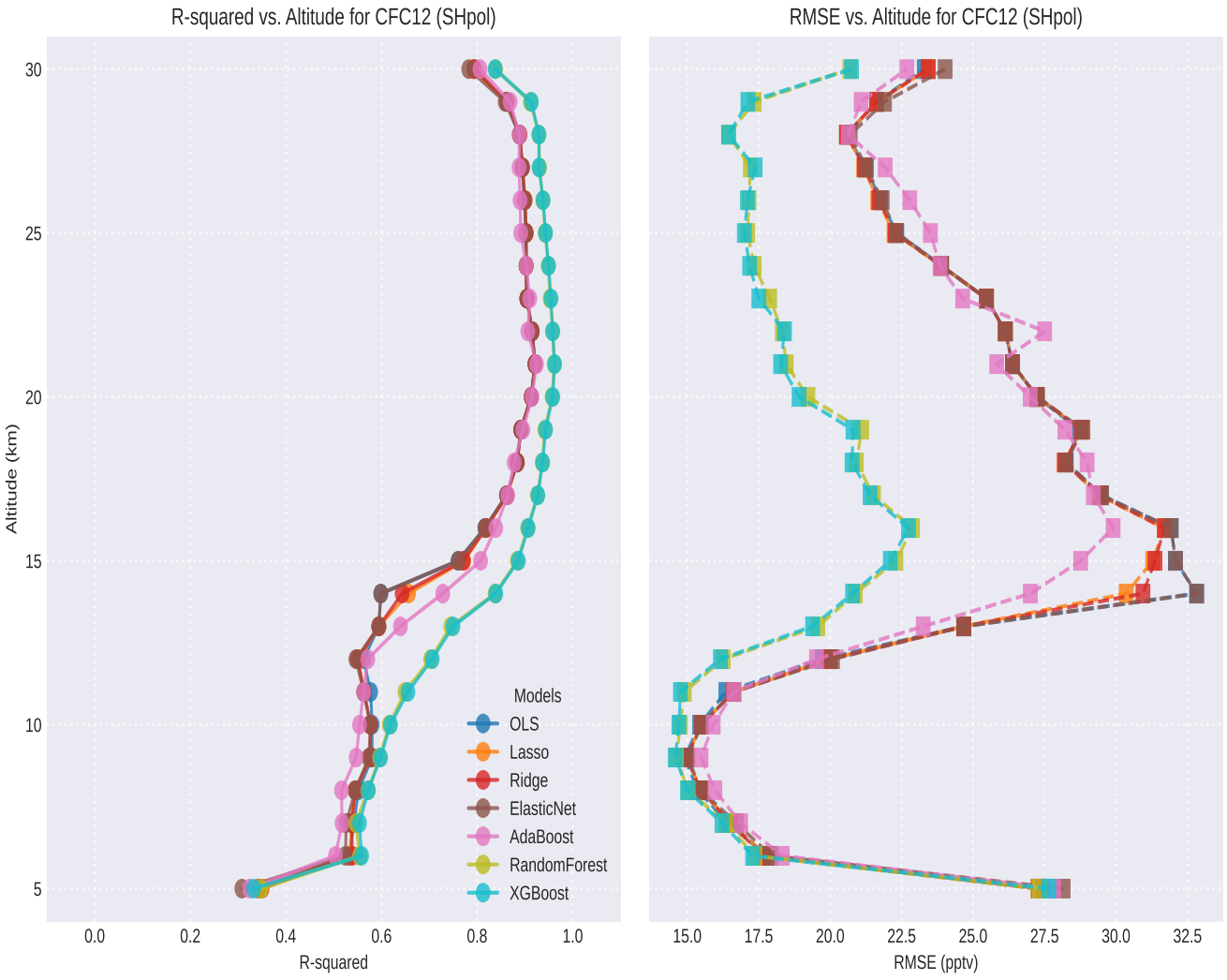

Figure S2. Same as Figure S1, but for CFC-12. Note the extended altitude range for CFC-12 (up to 30 km) relative to CFC-11 due to its longer atmospheric lifetime and higher photolysis altitude.

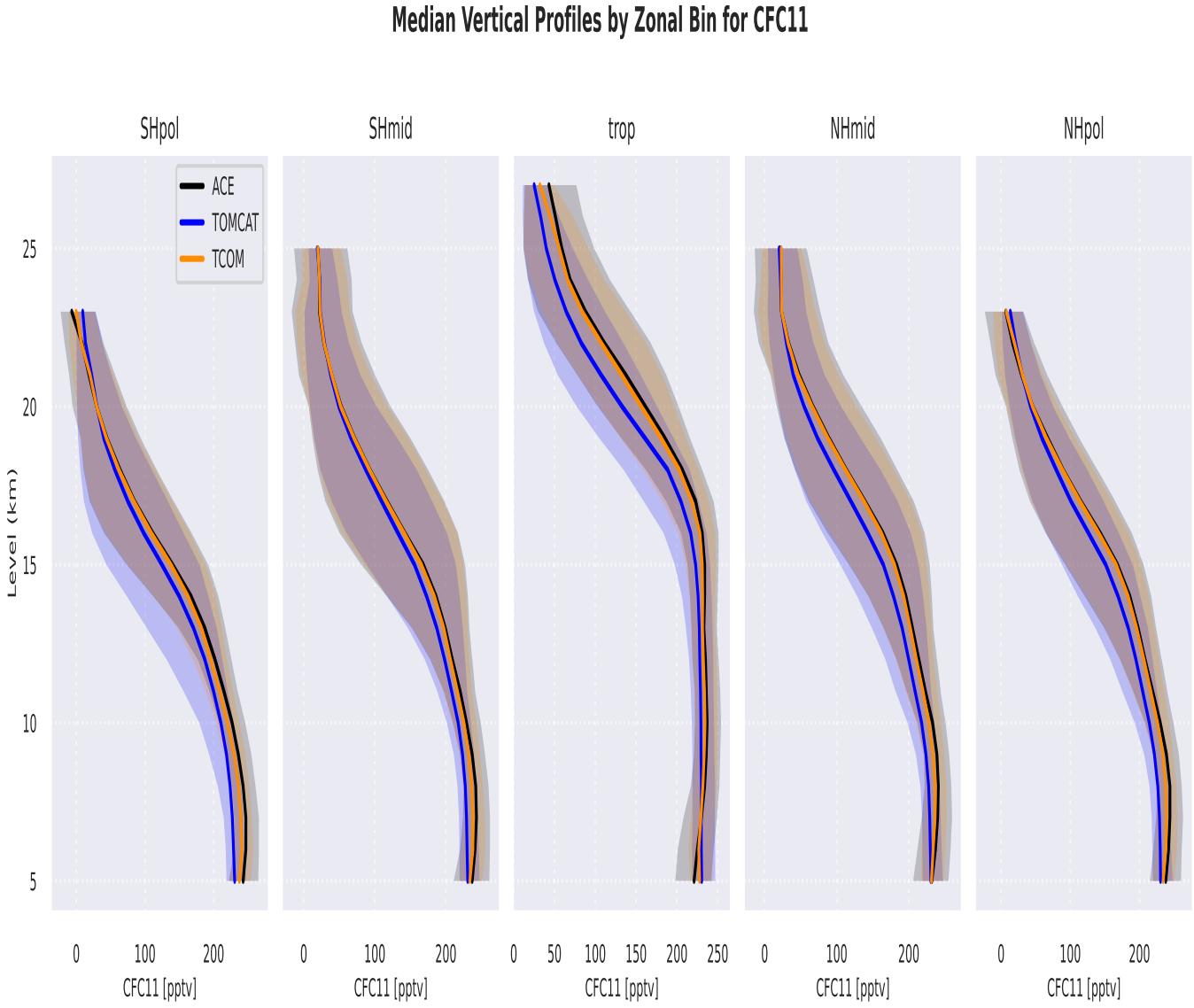

Figure S3. Comparison of median vertical profiles of CFC-11 for the five designated latitude bins: SHpol (90°S to 50°S), SHmid (70°S to 20°S), Trop (40°S to 40°N), NHmid (20°N to 70°N), and NHpol (50°N to 90°N). Profiles represent the TOMCAT background (blue), the XGBoost-corrected TCOM dataset (orange), and ACE-FTS satellite observations (black). Shaded regions represent the 10th to 90th percentile ranges, calculated exclusively using the 30% independent testing data.

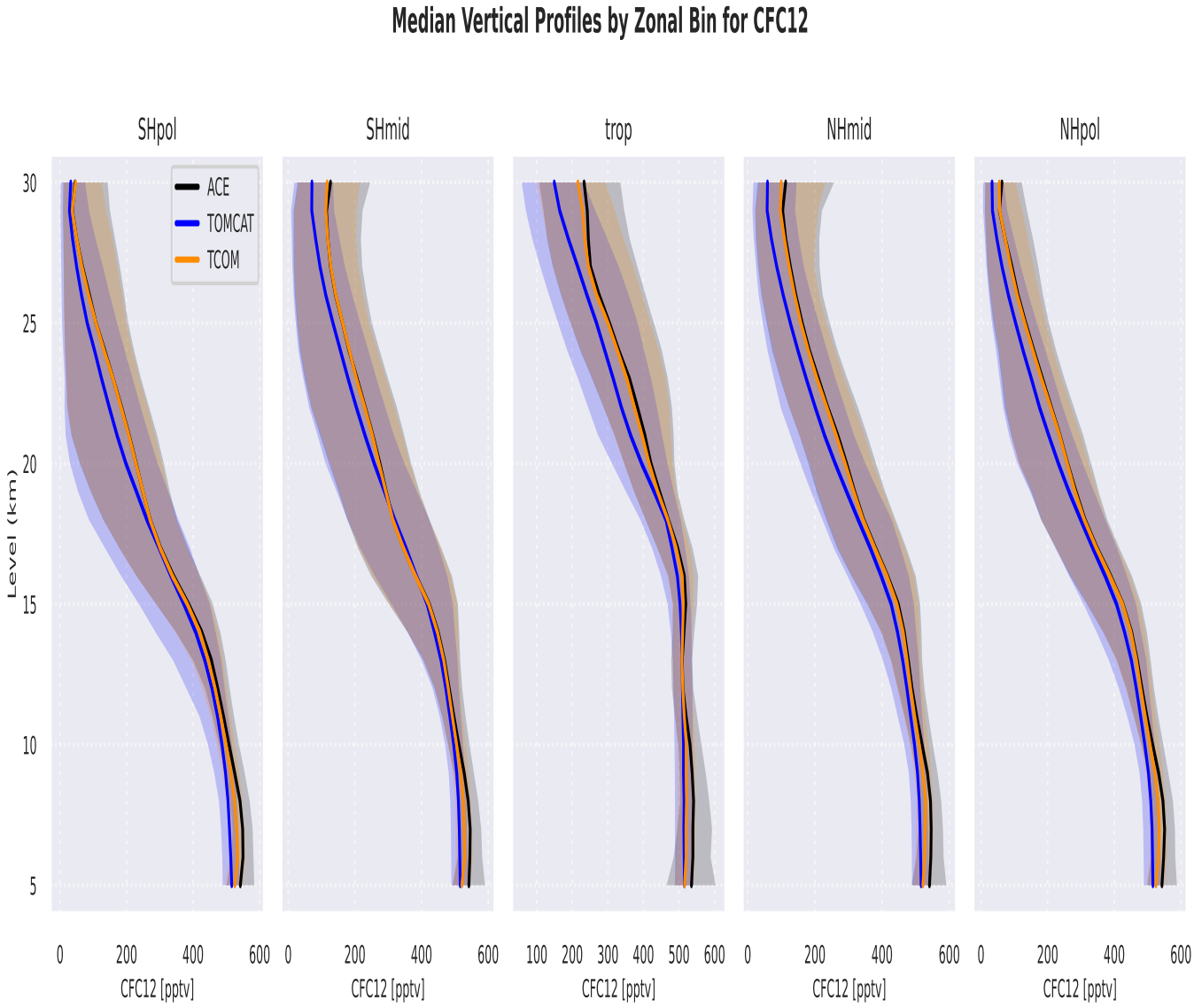

Figure S4. Same as Figure S3, but for CFC-12. These profiles confirm that the TCOM framework successfully removes the systematic low bias present in the raw TOMCAT simulations across all vertical levels.

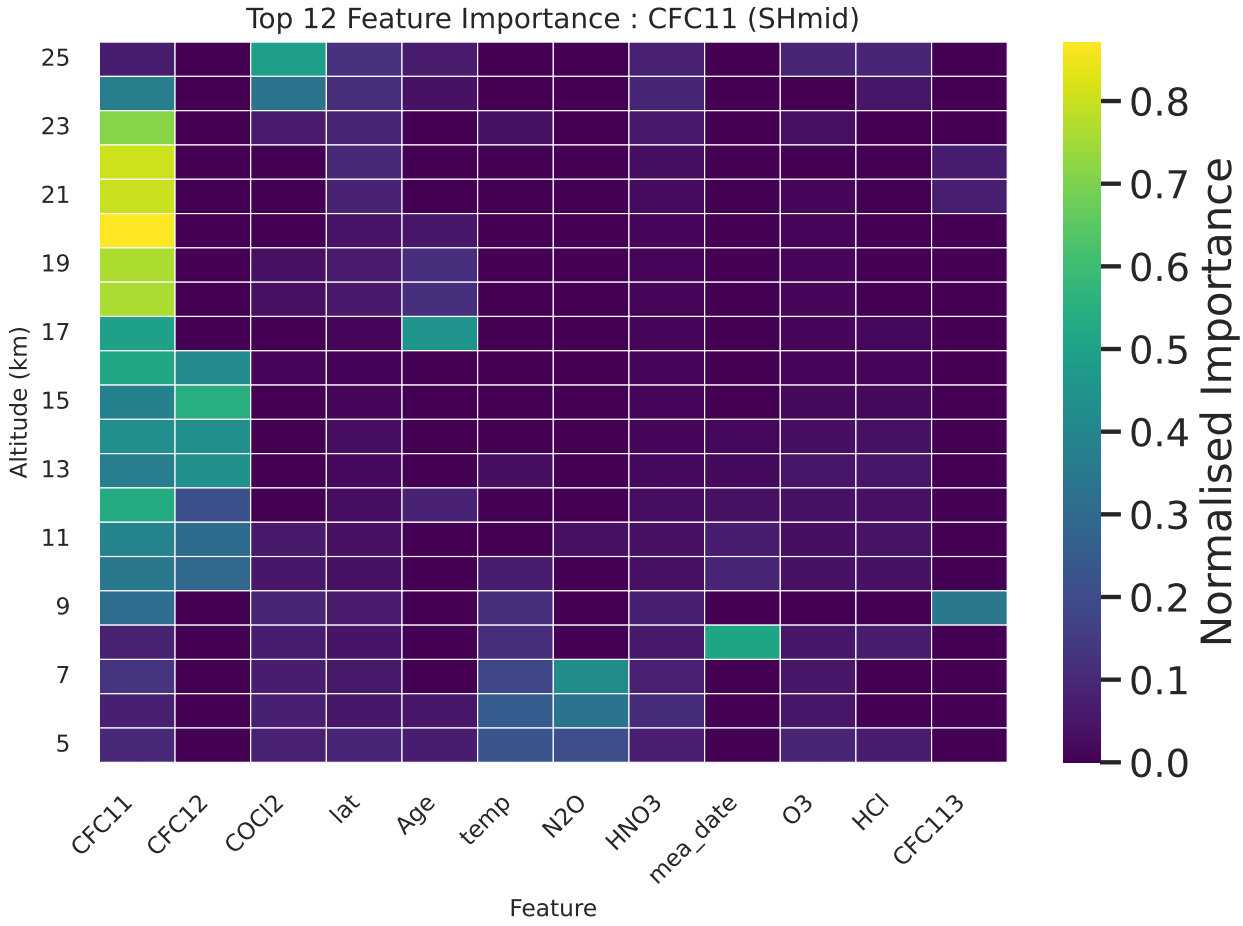

Figure S5. Normalised Feature Importance Heatmap for CFC-11 in the Southern Hemisphere mid-latitude (SHmid) latitude bin. The y-axis represents altitude (km) and the x-axis lists the 12 most important input features. Colour intensity indicates the relative importance of each feature in predicting the ACE-FTS VMRs. The dominance of the TOMCAT tracer suggests that fundamental transport and loss processes are well-represented in the CTM.

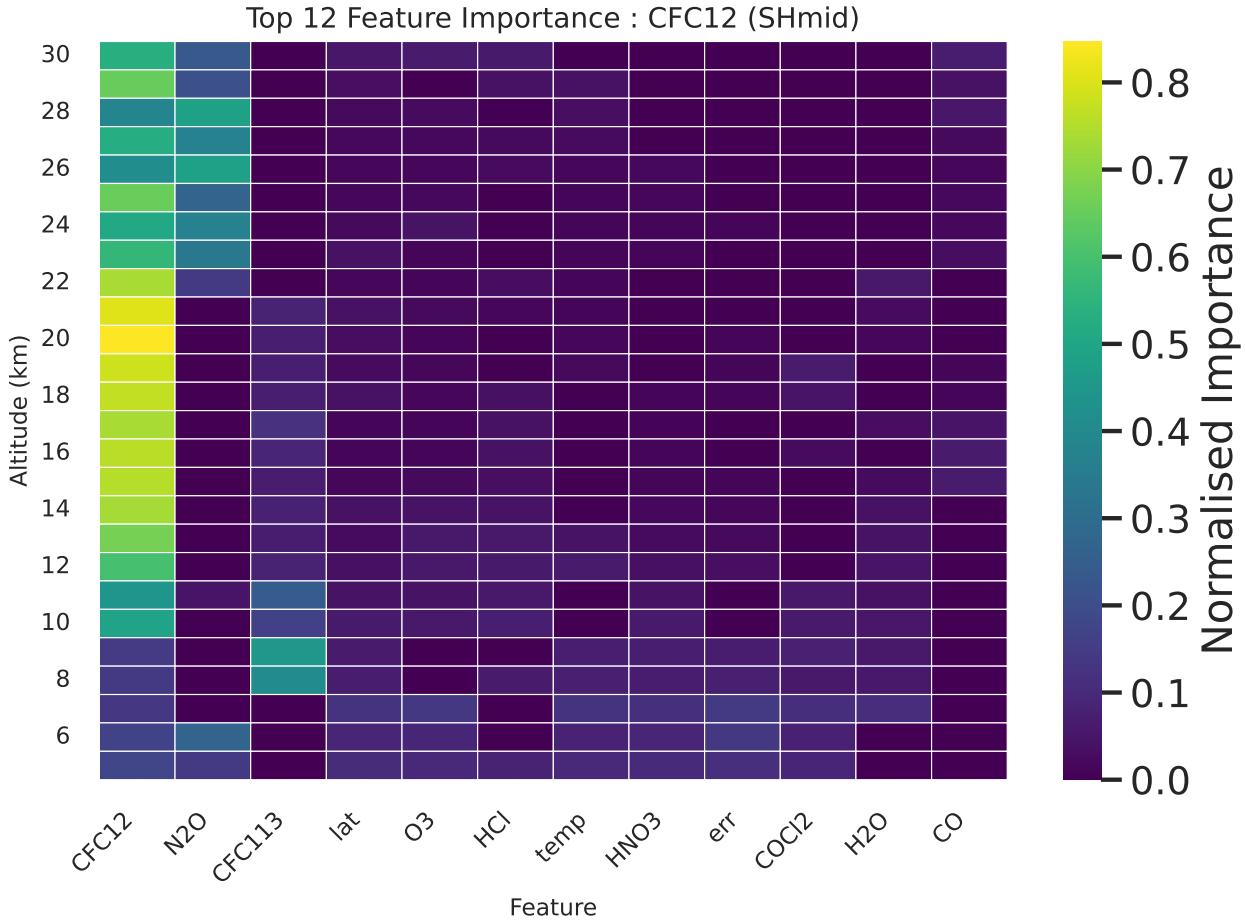

Figure S6. Same as Figure S5, but for the CFC-12 prediction in the SHmid latitude bin.

Figure S7. Same as Figure S5, but for CFC-11 in the Trop latitude bin. In the tropical UTLS, dynamical features and secondary tracers exhibit higher relative importance compared to high latitudes.

Figure S8. Same as Figure S5, but for CFC-12 in the Trop latitude bin.

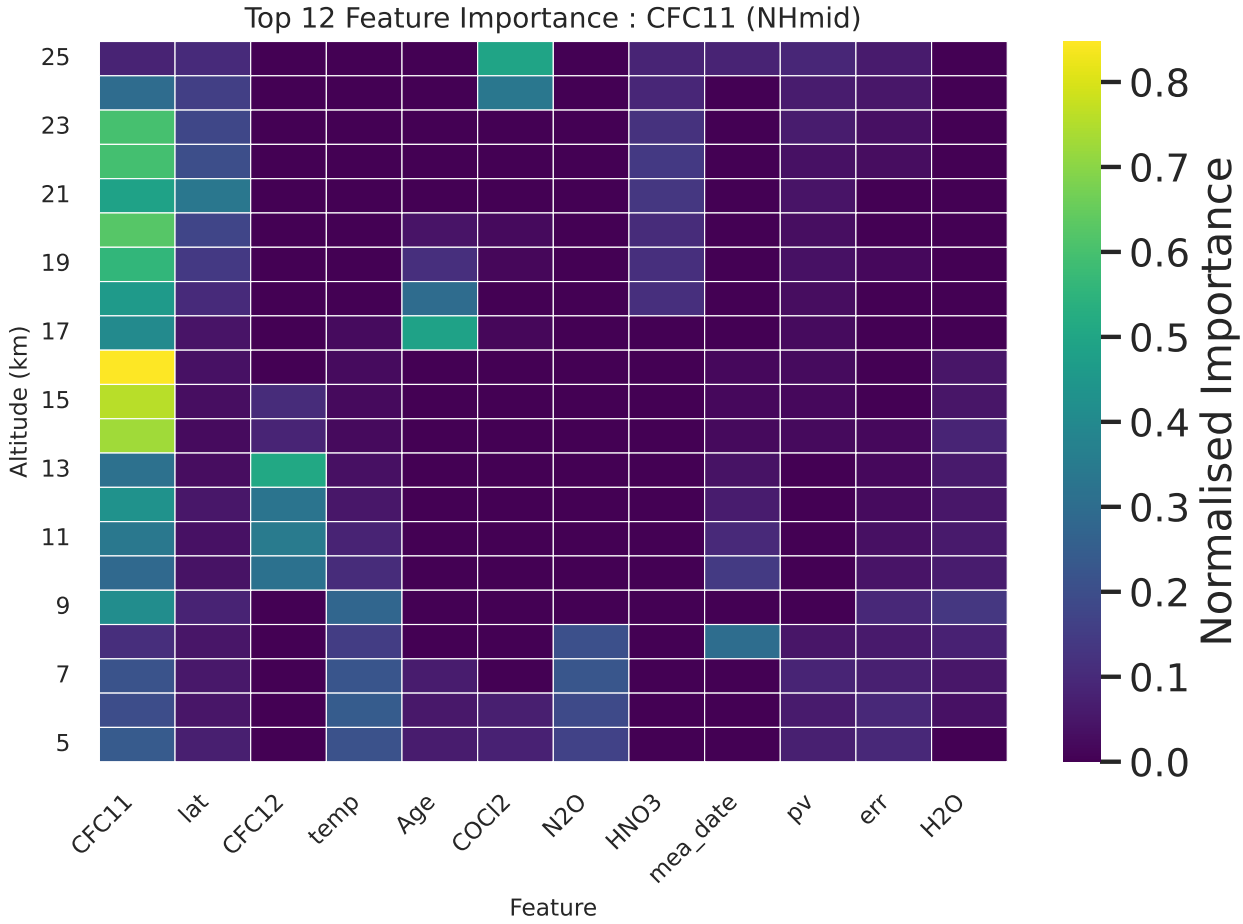

Figure S9. Same as Figure S5, but for CFC-11 in the NHmid latitude bin.

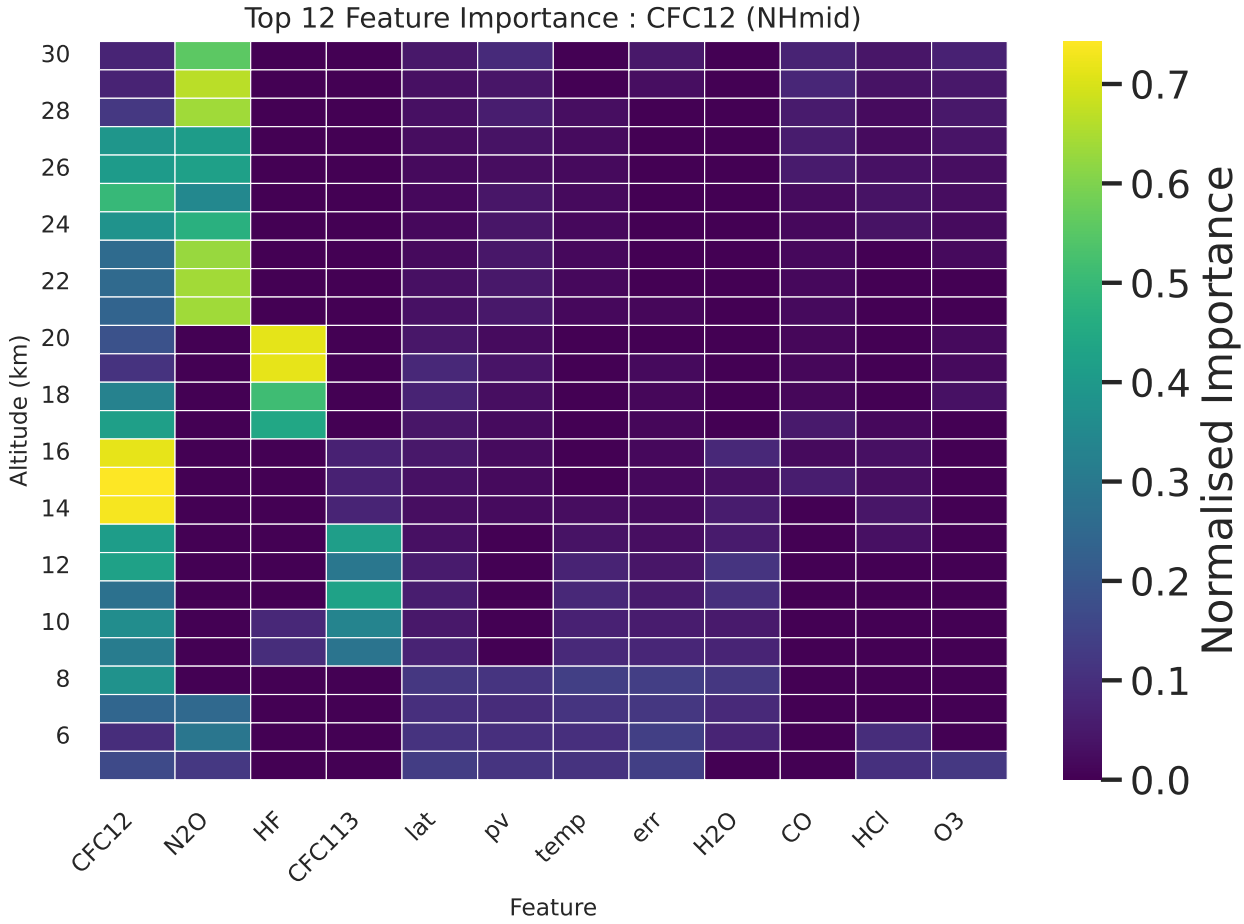

Figure S10. Same as Figure S5, but for CFC-12 in the NHmid latitude bin.

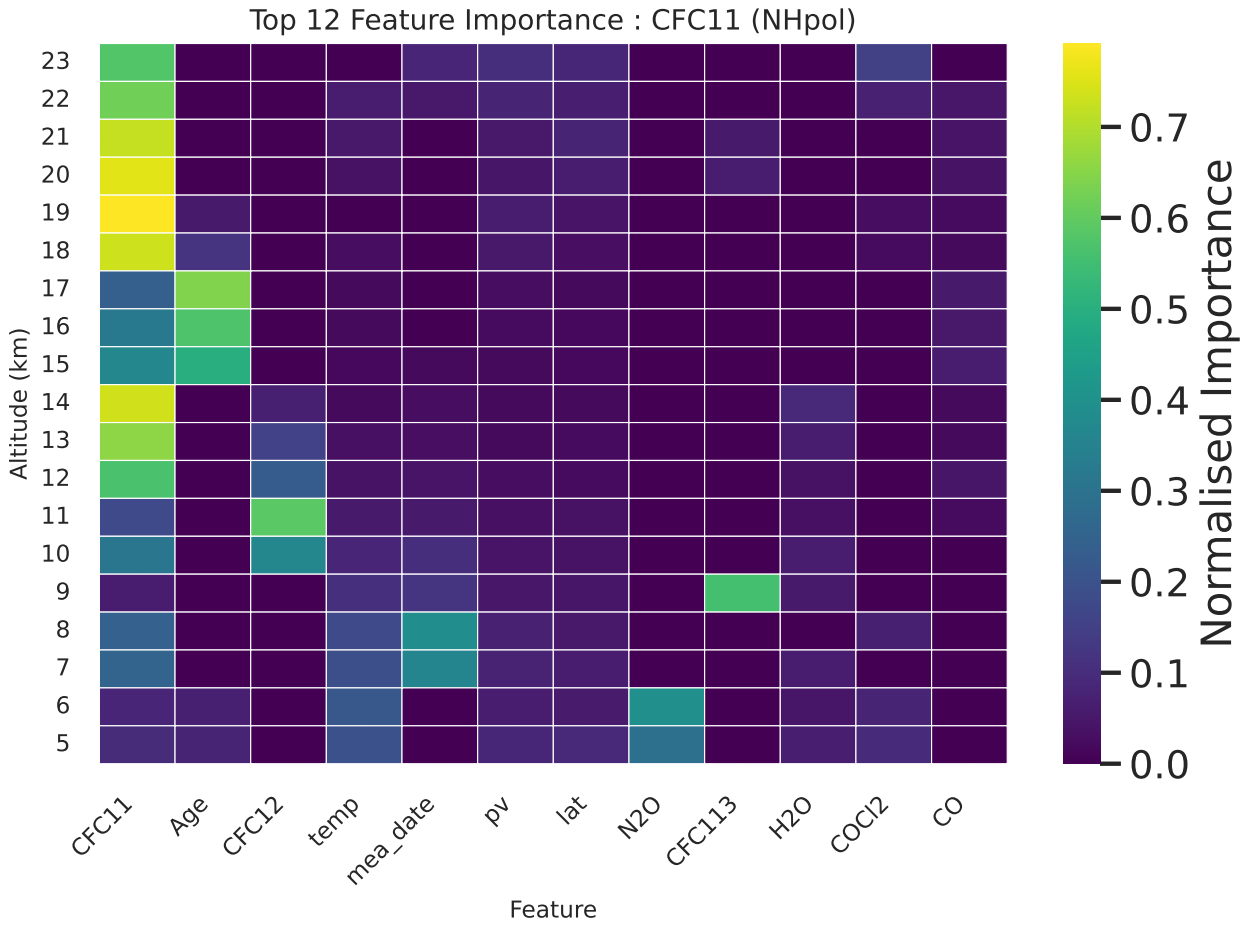

Figure S11. Same as Figure S5, but for CFC-11 in the NHpol latitude bin.

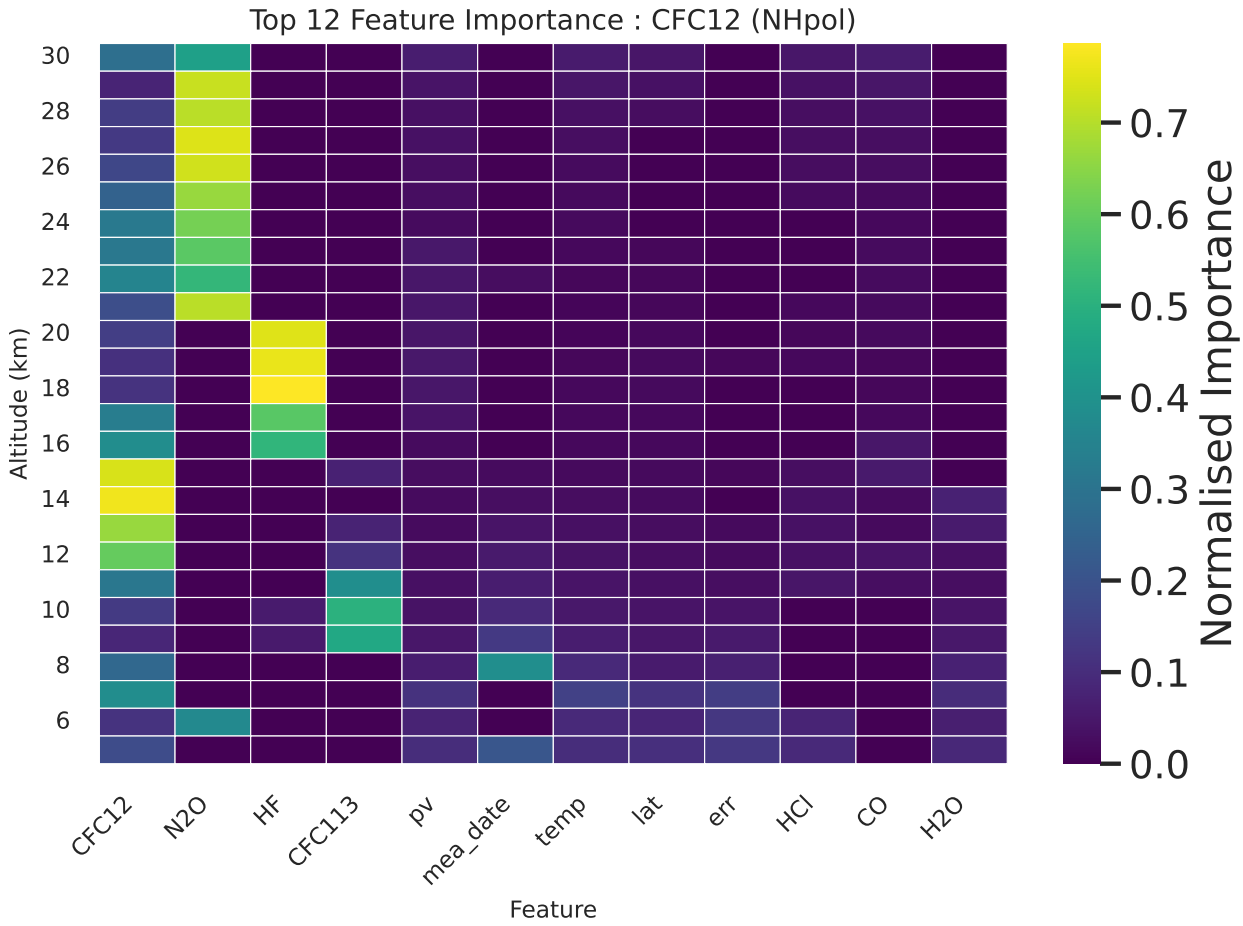

Figure S12. Same as Figure S5, but for CFC-12 in the NHpol latitude bin.

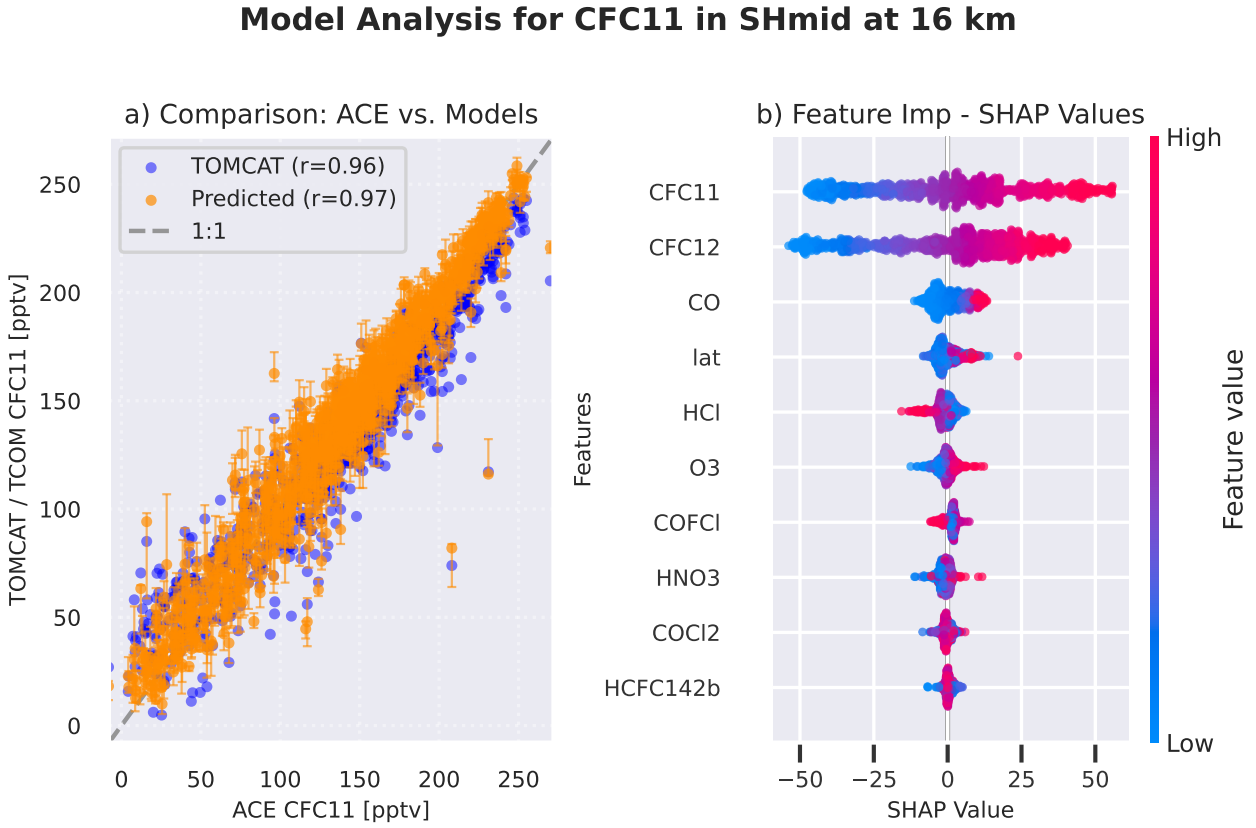

Figure S13. (a) Comparison of CFC-11 VMRs at 16 km altitude in the SHmid latitude band. Scatter plots compare co-located ACE-FTS observations against TOMCAT (blue) and XGBoost-predicted TCOM (orange). Vertical error bars on the TCOM data represent robust uncertainty estimates (σ_{TCOM}) derived from the 25th and 75th percentile ensemble retraining. **(b) SHAP values for CFC-11 at 16 km.** The values quantify the influence of individual features on the model prediction. High AoA (red dots) associated with negative SHAP values indicates a downward correction for aged, photochemically processed air masses.

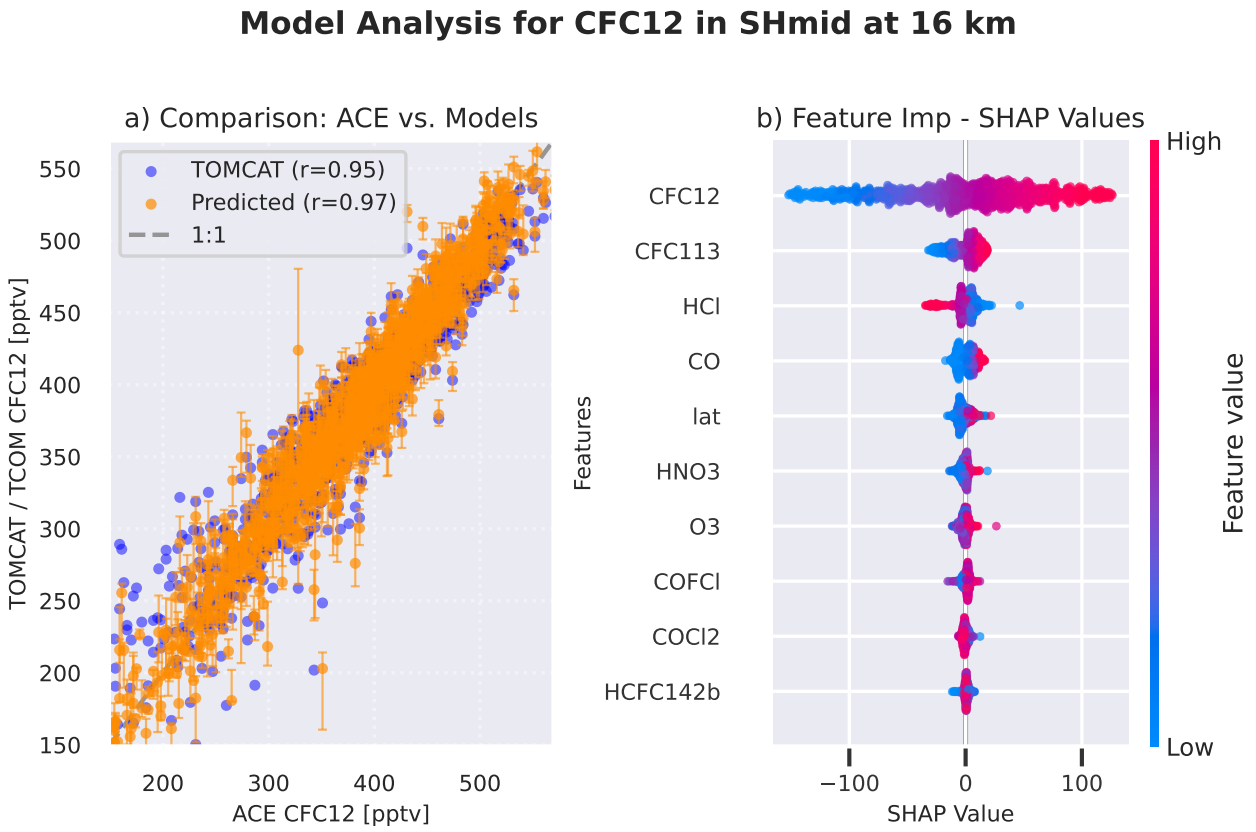

Figure S14. Same as Figure S13, but for CFC-12 at 16 km in the SHmid bin. The large positive corrections driven by cold temperatures (blue dots) illustrate the rectification of circulation-driven biases.

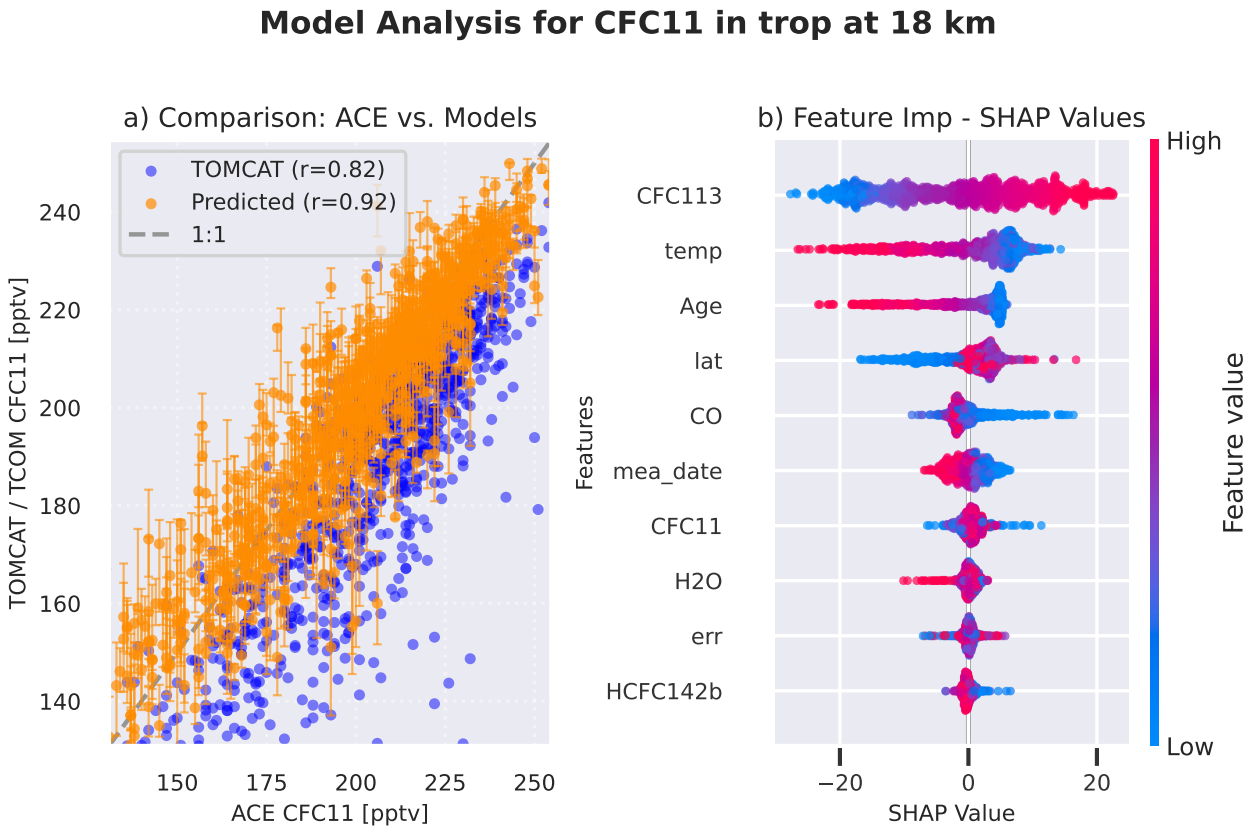

Figure S15. Same as Figure S13, but for CFC-11 at 18 km in the Trop latitude bin. Despite high dynamical variability and sparse observations, TCOM successfully resolves notable offsets in the tropical upper troposphere.

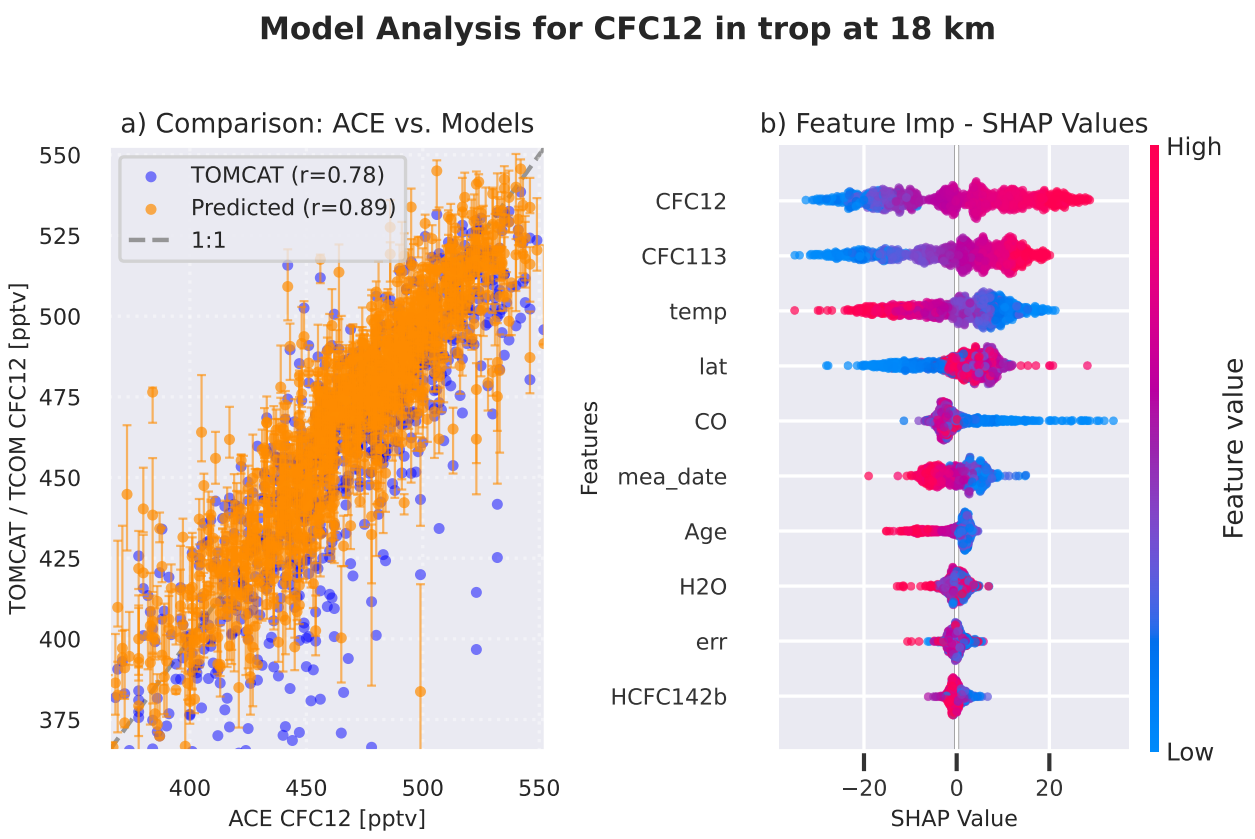

Figure S16. Same as Figure S13, but for CFC-12 at 18 km in the Trop bin.

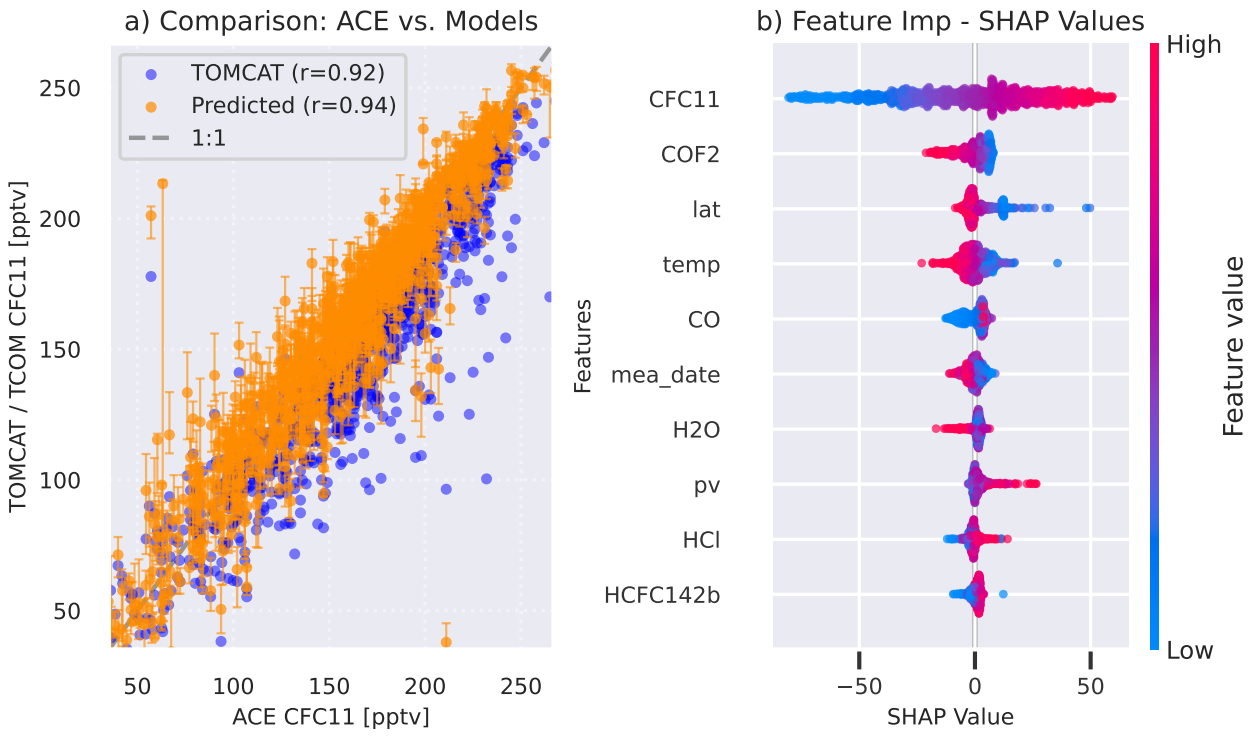

Figure S17. Same as Figure S13, but for CFC-11 at 16 km in the NHmid latitude bin.

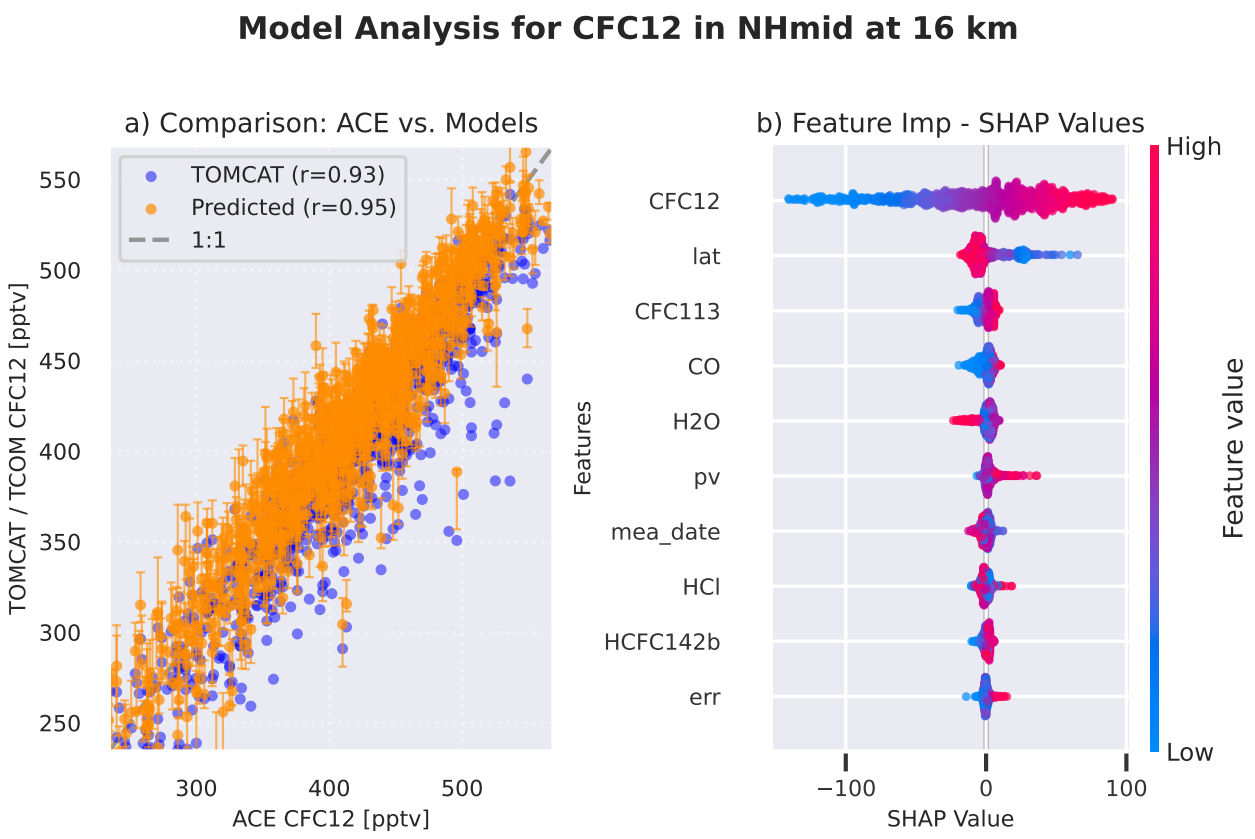

Figure S18. Same as Figure S13, but for CFC-12 at 16 km in the NHmid latitude bin.

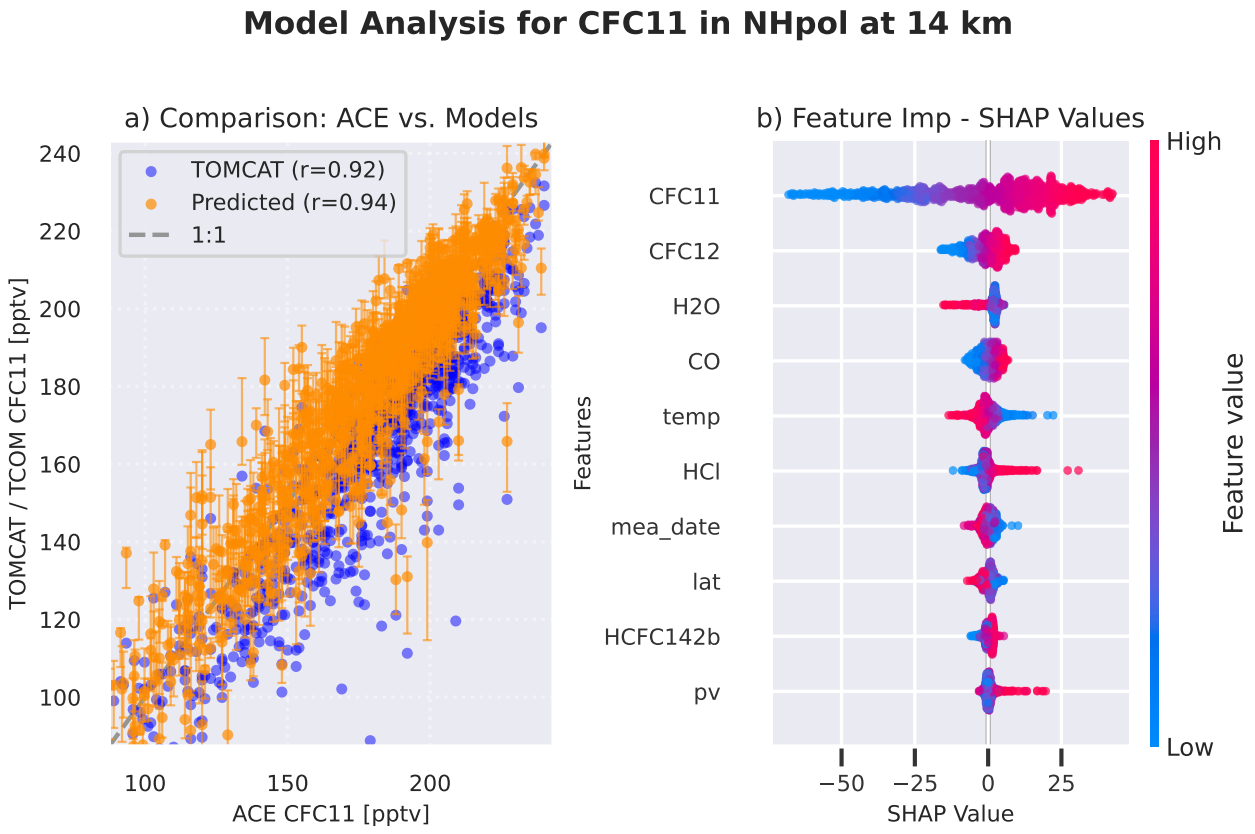

Figure S19. Same as Figure S13, but for CFC-11 at 14 km in the NHpol latitude bin. The negative SHAP values for high AoA confirm that TOMCAT tends to overestimate residual concentrations in wintertime subsided air.

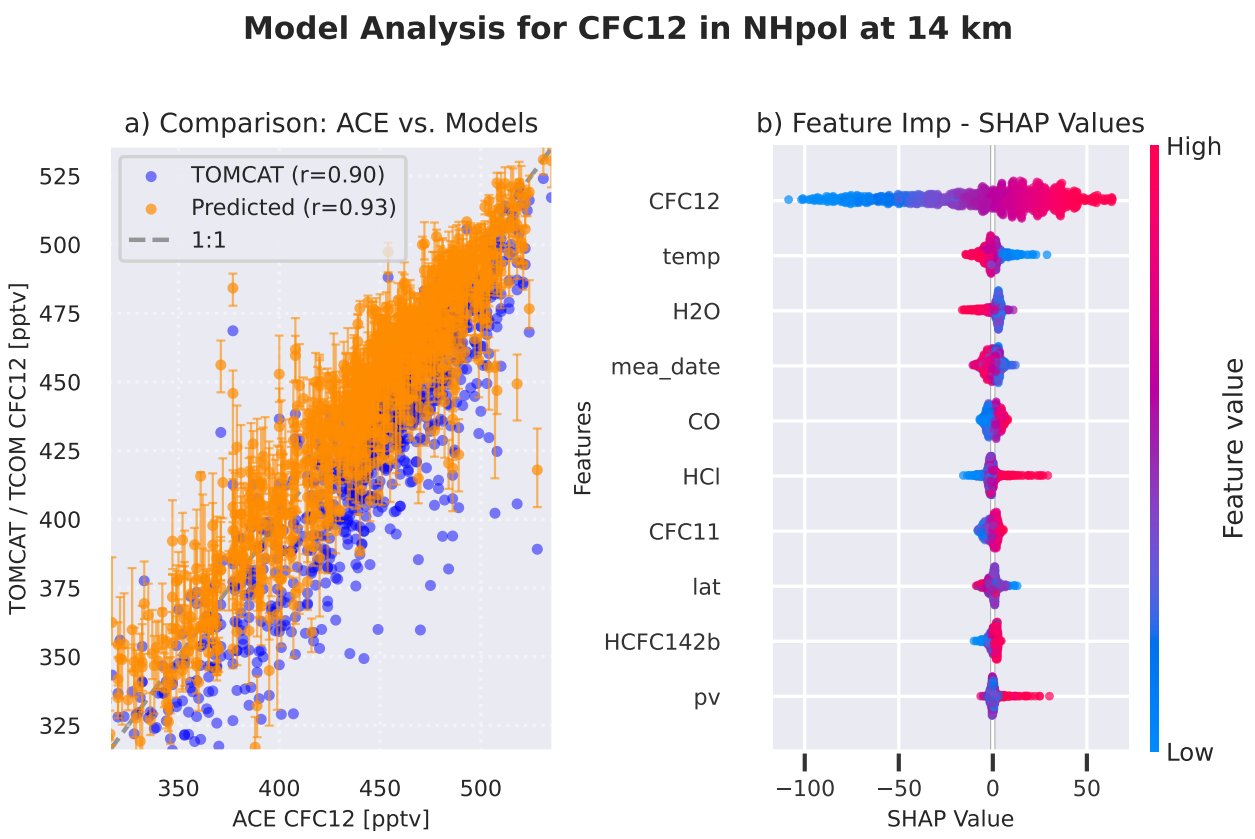

Figure S20. Same as Figure S13, but for CFC-12 at 14 km in the NHpol latitude bin.